Available online at www.sciencedirect.com
ScienceDirect
Biochimica et Biophysica Acta 1768 (2007) 1440–1447
Biochimica et Biophysica Acta BBA
www.elsevier.com/locate/bbamem

Role of hydrophobic residues in the voltage sensors of the voltage-gated sodium channel

Saïd Bendahhou [a], Andrias O. O'Reilly [b], Hervé Duclohier [c,*]

[a] Institut de Pharmacologie Moléculaire et Cellulaire, UMR 6097 CNRS, Université de Nice, Sophia Antipolis 660 Route des Lucioles, Sophia-Antipolis 06560 Valbonne, France
[b] Department of Crystallography, Birkbeck College, University of London, Malet Street, London WC1E 7HX, UK
[c] Institut de Physiologie et Biologie Cellulaires, UMR 6187 CNRS-Université de Poitiers, 40 Avenue du Recteur Pineau, 86022 Poitiers, France

Received 16 October 2006; received in revised form 7 February 2007; accepted 1 March 2007
Available online 15 March 2007

Abstract

The role of hydrophobic residues in voltage sensors S4 of voltage-sensitive ion channels is less documented than that of charged residues. We performed alanine-substitution of branched-sidechain residues contiguous to the third, fourth and fifth positively charged residues in S4s of the first three domains of the sodium channel expressed in HEK cells. These locations were selected because they are close to the arginines and lysines important in gating. Mutations in the first two domains (DIS4 and DIIS4) altered steady-state activation curves. In DIIIS4, the mutation L1131A next to the third arginine greatly slowed inactivation in a manner similar to that for substitutions of charged residues in DIVS4, whereas the mutation L1137A next to the fifth arginine preserved wild-type behaviour. Homology models of domain III, based on the structure of a crystallized mammalian potassium channel, shows that L1131 is located at the interface between S3 and S4 helices, whereas L1137, on the opposite side of S4, does not interact with the voltage sensor. The two mutated residues are closer to each other in domains I and II than in domain III, as may be corroborated by their different electrophysiological effects.

Keywords: Voltage sensors; Activation–inactivation coupling; Heterologous expression; Electrophysiology; Molecular modelling

1. Introduction

Voltage-gated potassium, sodium and calcium channels stochastically undergo conformational changes when cell membranes are depolarized. The á subunits of these channels are organized in four identical or homologous domains, each of which is composed of six transmembrane segments (S1–S6) with the pore region formed by the S5 and S6 segments and their connecting extracellular linker [1]. Voltage-gated potassium channels whose structure began to be solved to high resolution (through X-ray crystallography) in 1998 [2] are composed of four identical and independent subunits, whereas sodium and calcium channels are formed from a single large polypeptide chain with four homologous domains. One common feature of voltage-gated ion channels is the transmembrane segment S4, with positively charged residues (arginines and lysines) occurring every three amino acids and separated by two non-polar residues. This motif identifies the four S4 segments as critical components of the voltage sensor [3].

The first direct experimental evidence for their role in voltage sensing came from charge neutralizations within S4 segments, which led to reduction in gating current, alteration of channel conductance and kinetics, as well as shifts of the steady-state activation [3,4]. The second piece of evidence came from cysteine scanning mutagenesis experiments, which showed that S4 segments move their positive charges towards the extracellular face of the membrane upon depolarization [5,6]. Site-directed fluorescence labeling coupled to electrophysiology confirmed this outward movement, associated with a rotation of the S4s [7–9].

In voltage-gated sodium channels (for an overview of this family, see [10]), several naturally occurring mutations located in S4 segments cause either paramyotonia congenita [11,12] or hypokalemic periodic paralysis [13,14]. The functional consequences of these mutations were assessed in myotubes or in heterologously expressing cells. Many defects were reported in

* Corresponding author. Tel.: +33 549 366 399; fax: +33 549 454 014.
E-mail address: Herve.Duclohier@univ-poitiers.fr (H. Duclohier).

0005-2736/$ - see front matter © 2007 Elsevier B.V. All rights reserved.
doi:10.1016/j.bbamem.2007.03.002

channel fast inactivation, recovery from inactivation and deactivation of the sodium channel [15], as well as a reduced current density in the calcium channel [16]. Another study reports the involvement of the middle region of the S4 segment of sodium channel domain IV in slow inactivation [17]. Most of the studies devoted to S4s in voltage sensors thus focused on arginines and lysines to elucidate the molecular mechanism of the voltage-sensitive ion channel gating. However, a substitution of a neutral amino acid at position 860 (specifically Phe→Leu) in S4 of domain II of the rat isoform of the sodium channel was shown to shift the current–voltage relationship by 20–25 mV in the depolarizing direction, i.e. activation was altered significantly, and the closed state favoured whereas inactivation remained unaffected. The activation shift is approximately equivalent to the one observed with the combined neutralization of two positive charges flanking the leucine 860 [18]. Lopez and colleagues showed that hydrophobic mutations in the segment S4 modify voltage-dependent gating in the *Shaker* potassium channel. Shifts of steady-state activation and/or inactivation curves caused by substitutions of hydrophobic residues in the S4 segment were comparable or even larger than with S4 basic charged residues [19].

The present study was partly motivated by reports of the unusual dielectric properties in liquid crystals composed of molecules with branched hydrophobic amino-acid sidechains [20], as applied to the structure–function relations of voltage-sensitive ion channels [21]. We show here that substitution of branched amino acid residues with unbranched residues in S4 segments in the first three domains of the voltage-dependent sodium channel have quite significant effects on activation or inactivation parameters depending on which domain is considered. These substitutions produced similar effects as seen when charged amino acids in the voltage sensor are replaced with neutral residues, supporting the idea that an energetic balance between hydrophobic and electrostatic interactions is important for the gating function of S4s [22–24].

Our initial peptide approach [25] already suggested a role for hydrophobic residues with branched vs. chiral sidechains. We then studied the contribution of the hydrophobic residues in voltage gating by replacing phenylalanines or leucines adjacent to arginine or lysine residues in S4s of domains I, II and III with alanines. Here we show that reducing the sidechain size of the hydrophobic amino acid has a significant effect on channel gating, similar to that seen for substitutions of the charged residues located at the outer vestibule. Finally, the structure of the crystallized rat brain Kv1.2 channel, a member of the *Shaker* family of voltage-gated potassium channels solved to 2.9 Å resolution by X-ray crystallography [26], is used here for homology modelling of domains I, II, and III voltage sensors of Nav1.4, adopting the activated conformation.

2. Materials and methods

2.1. Cell culture and transfection. Construction of Nav1.4 mutants

Human embryonic kidney (HEK 293) cells were grown and maintained as previously described [27] in 100-mm culture dishes at 37 °C under 5% CO_2. The calcium-phosphate precipitation technique was employed [28].

Human skeletal muscle sodium channel cDNA clone was used as a template to engineer three mutations by the megaprimer PCR method of site-directed mutagenesis [29]. To engineer the L224A, L227A, L674A, F677A, L1131A, L1137A and L1131P mutations, reactions were primed using oligonucleotides described in Table 1. For the L1131A mutation, Nav 1.4 L1131P construct was used as a template. The primers contained nucleotide substitutions as indicated in bold face. The protocol for the first round of PCR was: 2 min at 94 °C for one cycle; 20 s at 94 °C, 20 s at 50 °C, and 2 min at 72 °C for 30 cycles; and 5 min at 72 °C for one cycle. The following protocol was applied during the second round of PCR: 2 min at 94 °C for one cycle, 20 s at 94 °C, 20 s at 60 °C, and 4 min at 72 °C for 30 cycles; and 10 min at 72 °C for one cycle.

All PCR reactions were carried out in DNA Engine Tetrad (MJ Research, Watertown, Massachusetts, USA). DNA Sequencing was performed using either ABI Rhodamine dye terminators, or ABI Prism BigDye Terminators and cycle sequencing with Taq FS DNA polymerase. DNA sequence was collected and analyzed on an ABI Prism 377 automated DNA sequencer (Perkin-Elmer Applied Biosystems, Foster City, California, USA). Primers were synthesized on a 394 automated DNA synthesizer (Perkin-Elmer Applied Biosystems) following standard ABI procedures.

2.2. Patch clamp recordings, voltage protocols and data analysis

Recordings were conducted in the whole-cell configuration [30] at room temperature (22 °C). Thirty-six hours after transfection, culture media was replaced with the bathing solution: 140 mM NaCl, 4 mM $MgCl_2$, 2 mM $CaCl_2$, and 10 mM Na–HEPES at pH 7.3. The internal pipette solution contained: 130 mM CsCl, 4 mM $MgCl_2$, 2.5 mM EGTA, 5 mM NaCl, and 10 mM HEPES at pH 7.3.

Peak Na^+ conductance (GNa) was measured during a 25-ms depolarization to various test potentials from a holding potential of −120 mV to characterize steady-state activation. GNa is calculated from the relation GNa=INa/(V−Vrev), where INa is the peak inward Na^+ current during the test depolarization (V) and Vrev is the Na^+ reversal potential. Data are normalized to maximum peak conductance (Gmax) and fitted to a two-state Boltzmann distribution

$$\mathrm{GNa/Gmax} = (1 + \exp[ze(V - V_{1/2})/kT])^{-1}$$

where $V_{1/2}$ is the test potential for half-maximal Na^+ activation, z the apparent gating charge, k the Boltzmann constant, T the absolute temperature (kT/e=25 mV at 22 °C). To study steady-state fast inactivation, cells were held at prepulse potentials ranging from −140 mV or −120 mV to +20 mV for 200 ms, then subjected to a 0 mV test pulse for 25 ms. Normalized peak currents were plotted versus prepulse potentials, and curves were fitted by the Boltzmann function as described above, applied for I/Imax, where Imax is the current recorded at 0 mV following the most hyperpolarizing prepulse. Tail currents were elicited by a 0.5 ms test pulse to +40 mV followed by a repolarization pulse ranging from −120 mV to −40 mV. Resulting currents were fitted by a single-exponential decay and expressed as a function of the voltage.

2.3. Molecular modelling

Homology models of the Nav1.4 domains I–III voltage sensors were generated using the crystal structure of the rat brain Kv1.2 voltage-gated *Shaker* potassium channel (Protein Data Bank code 2A79) [31] as the structural template. The amino-acid sequences of the sodium (Swiss-Prot accession P35499) and potassium (Swiss-Prot accession P63142) channels were aligned using the ClustalW algorithm [32]. Residues in the potassium channel structure were mutated using the SYBYL modelling software (Version 7.0, Tripos Inc.). The sodium channel models were subjected to 100 steps of conjugate gradient energy minimization in SYBYL using the Tripos force-field [33]. Rotamers were chosen in SYBYL for the sidechains of charged residues on the S2, S3 and S4 helices in order to maximise the number of salt bridges in the voltage sensor models; oppositely charged atoms 4 Å apart were considered to form a salt bridge. The models were subjected to another 100 steps of conjugate gradient energy minimisation in SYBYL. Figures were

Table 1
Primers used in PCR reactions to engineer Nav1.4 mutant constructs

Mutations	First round PCR primers (5′ to 3′)	Second round PCR primers (5′ to 3′)
L224A	CATCTCTGTGCACCCTGGCT	CATCTCTGTGCACCCTGGCT
	GTTTTGAGGGCCCGC**GC**CAC	ATCCGAGGCTGCCAGACTGT
	GTG**GC**GCGGGCCCTCAAAAC	and 2 megaprimers from 1st round PCR
	ATCCGAGGCTGCCAGACTGT	
L227A	CATCTCTGTGCACCCTGGCT	CATCTCTGTGCACCCTGGCT
	CTGCGGGCC**GC**CAAAACCAT	ATCCGAGGCTGCCAGACTGT
	ATGGTTTTG**GC**GGCCCGCAG	and 2 megaprimers from 1st round PCR
	ATCCGAGGCTGCCAGACTGT	
L674A	CATGAGTGACCCGCCTCCCT	CATGAGTGACCCGCCTCCCT
	AGACCCGC**GC**CAGACGGAAG	CTCGGGCGGCTCCTTCTTCT
	CTTCCGTCTG**GC**GCGGGTCT	and 2 megaprimers from 1st round PCR
	CTCGGGCGGCTCCTTCTTCT	
F677A	CATGAGTGACCCGCCTCCCT	CATGAGTGACCCGCCTCCCT
	GCCAGCTTG**GC**GACCCGCAG	CTCGGGCGGCTCCTTCTTCT
	CTGCGGGTC**GC**CAAGCTGGC	and 2 megaprimers from 1st round PCR
	CTCGGGCGGCTCCTTCTTCT	
	CCACTCCTTCCTCATCGTCTTCCGCAT	CCACTCCTTCCTCATCGTCTTCCGCAT
L1131P	AGGGCCCGC**G**CTGTCCGGAGGGATTTGAT	GATGATGCTGTTGCCGAAGGTCTCGAA
	ATCAAATCCC**C**TCCGGACAC**C**GCGGGCCCT	and 2 megaprimers from 1st round PCR
	GATGATGCTGTTGCCGAAGGTCTCGAA	
	CCACTCCTTCCTCATCGTCTTCCGCAT	CCACTCCTTCCTCATCGTCTTCCGCAT
L1131A	AGGGCCCGCGCTGTCCGGAGGGATTTGAT	GATGATGCTGTTGCCGAAGGTCTCGAA
	ATCAAATCCCTCCGGACAGCGCGGGCCCT	and 2 megaprimers from 1st round PCR
	GATGATGCTGTTGCCGAAGGTCTCGAA	
L1137A	CCACTCCTTCCTCATCGTCTTCCGCAT	CCACTCCTTCCTCATCGTCTTCCGCAT
	AATCGGGACAGTGCCCTC**GC**GGGACGCA	GATGATGCTGTTGCCGAAGGTCTCGAA
	TGCGTCCC**GC**GAGGGCACTGTCCCGATT	and 2 megaprimers from 1st round PCR
	GATGATGCTGTTGCCGAAGGTCTCGAA	

produced using the PyMol molecular graphics system (DeLano Scientific, San Carlos, CA, USA).

3. Results

Human skeletal muscle sodium channel gene *SCN4A* was introduced into HEK293 cells and expression was monitored using the whole cell voltage clamp technique. Alanine substitutions of hydrophobic residues with branched sidechains was applied to engineer six mutations in the WT *SCN4A* cDNA in order to study their effect on channel gating. These mutations (five leucines and a phenylalanine), adjacent to arginines previously found as the most important in voltage sensing (*e.g.* the third arginine from the left in Fig. 1) or lysines are located in S4 segments of domains I, II and III. They were changed to alanine, a small side chain residue thus reducing the steric effect of the bulky Leu/Phe. We investigated kinetics changes and voltage dependencies of all constructs and compared their behaviour to that of wild-type (WT) channels.

3.1. Mutations in DI and DII affect steady-state activation

Current recordings from cells expressing either L224A or L227A in DIS4, L674A, or F677A in DIIS4 showed activation and inactivation kinetics nearly similar to those recorded with WT channels (Fig. 2A and B). Despite a small but non-significant slow inactivation component developing, fast inactivation decay was unaffected. The steady-state inactivation showed no shift in the voltage-dependence of all mutants compared to WT. However, as seen in these panels, steady-state activation curves were affected for all of the mutants. While substitutions L227A, L674 and F677A shifted the activation curve to depolarizing voltages, favouring the channel closed state, for L224A there was a left shift to hyperpolarizing voltages that enhances the channel open state (Table 2). Channel deactivation was not altered in the mutant constructs and

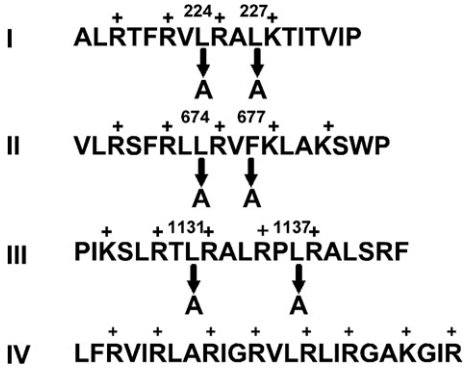

Fig. 1. Mutations of hydrophobic residues to alanine in S4s of the first three domains of the voltage-gated channel. In the amino-acid sequence of the four segments S4 of the human skeletal muscle Na^+ channel Nav1.4, positively charged residues are shown with a + sign and hydrophobic residues that are mutated to alanine are numbered 224, 227, 674, 677, 1131, and 1137.

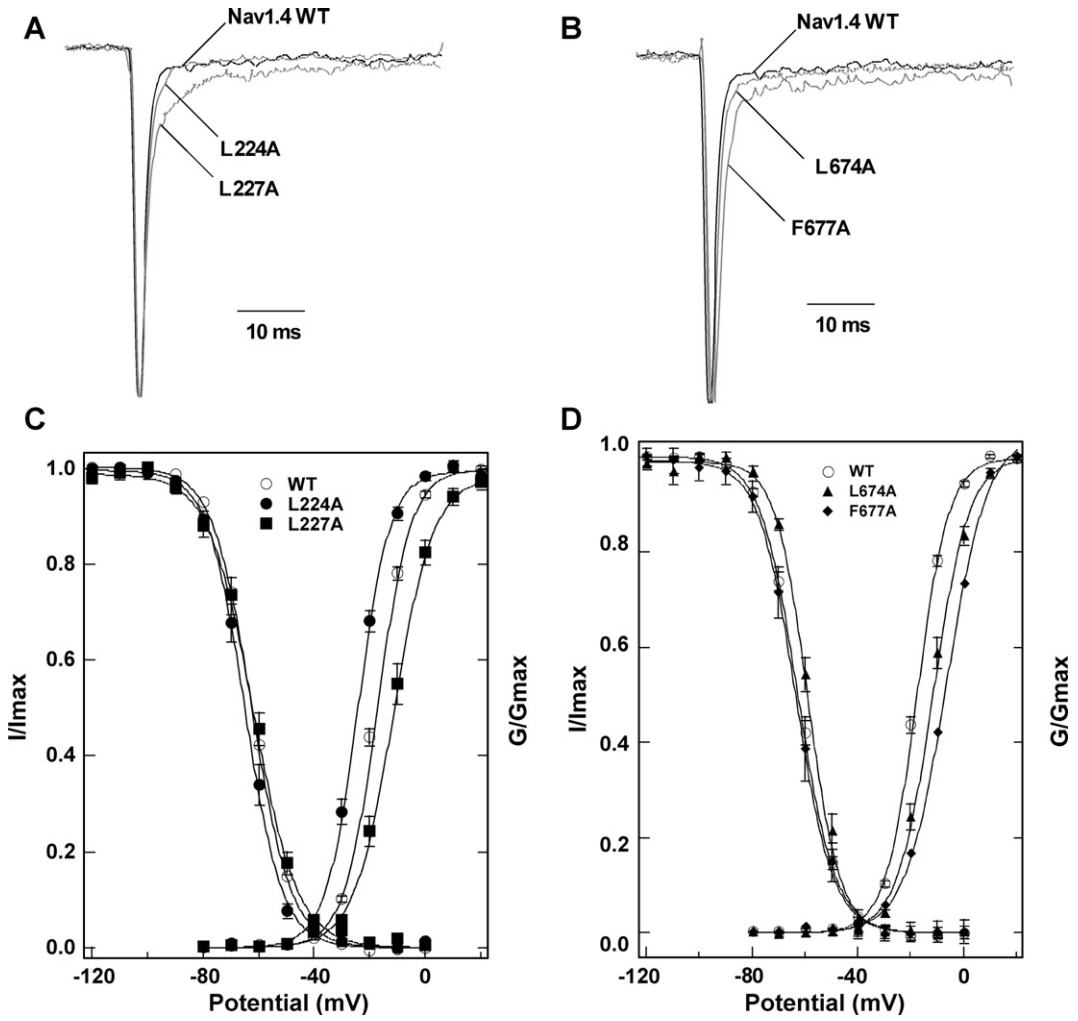

Fig. 2. Substitutions in DI and DII voltage sensors affect channel activation. Representative whole cell current traces recorded at −10 mV from HEK293 cells transfected with WT, L224A, L227A (A), L674A or F677A (B). Traces were normalized to show the activation and inactivation kinetics of the mutated channels at a comparable scale to those of WT channels. Steady state activation (C) and inactivation (D) for WT (open circles), L224A (filled circles), L227A (filled squares), L674A (filled triangles), and F677A (filled diamonds) channels in HEK293 cells. Protocols are as described in Materials and methods. Values are mean±S.E.M.

recovery from inactivation was not affected at −120 mV and −100 mV but was slightly enhanced at −80 mV.

3.2. Mutations in DIIIS4 mainly affect channel inactivation and slightly delay time-to-peak of sodium current

Whole cell inward current at −10 mV showed that L1131A channels exhibited slower inactivation kinetics (Fig. 3A) whereas L1137A mutant channels had similar inactivation kinetics to that of WT channels. As evidenced by the slightly delayed peak with the L1131A substitution, there is also an effect on activation kinetics. At the same voltage, the time constant for fast inactivation of L1131A is about 3–4 times slower than that of WT channels (Fig. 3C). The steady-state fast inactivation was shifted toward hyperpolarizing potentials for both mutations (Fig. 3B). This shift was accompanied by a reduction of the slope factor significant only for the L1131A channels (for WT, $z=-3.9\pm0.7$, $n=43$; L1131A, $z=-2.1\pm0.2$, $n=13$; and for L1137A, $z=-3.8\pm0.1$, $n=9$). Holding the cells at a more hyperpolarizing potential (−140 mV) for the L1131A mutant did not affect significantly these values ($V_{1/2}=-70.5\pm2.2$ mV, $z=-2.2\pm0.1$, $n=7$). These electrophysiological data, normalized taking into account different current densities in cells, are summarized in Table 2. It should be noted that except for the L1131P mutation (outside the scope of the present study) for which a reduction of the sodium current was observed, the peak inward current remained unaffected by these mutations.

Table 2
Activation and fast inactivation parameters for Nav1.4 variants

Clone	Activation $V_{1/2}$ (mV)	Activation slope	Fast inactivation $V_{1/2}$ (mV)	Fast inactivation slope
WT	−17.7±0.4 (47)	3.8±0.5 (28)	−62.1±0.7 (43)	−3.9±0.7 (26)
L224A	−24.5±1.2 (13)	4.1±0.6 (13)	−65.1±1.2 (10)	−4.5±0.1 (10)
L227A	−11.3±0.4 (8)	2.9±0.7 (7)	−62.2±1.1 (13)	−3.4±0.2 (12)
L674A	−10.7±0.7 (13)	3.5±0.5 (13)	−58.0±0.7 (13)	−3.8±0.1 (11)
F677A	−6.2±1.3 (9)	3.8±0.4 (8)	−61.6±1.5 (10)	−3.9±0.2 (8)
L1131A	−18.5±0.9 (12)	3.5±0.5 (12)	−70.8±1.9 (20)	−2.1±0.2 (13)
L1137A	−18.9±1.5 (8)	3.2±0.3 (8)	−67.6±1.5 (9)	−3.8±0.1 (9)

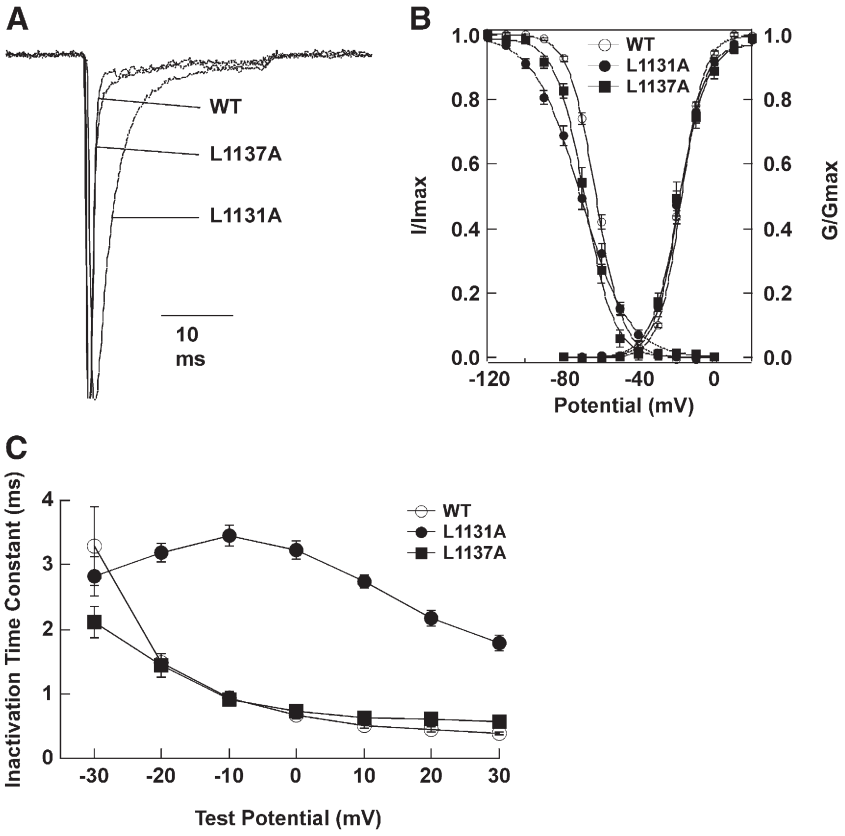

Fig. 3. Substitutions in DIII voltage sensors affect channel fast inactivation strongly and activation slightly. Whole cell current traces at −10 mV from HEK293 cells transfected with either WT, L1131A or L1137A (A). Traces were normalized to show the differences in current decay. (B) Voltage dependence of activation and inactivation for WT (open circles), L1131A (filled circles), and L1137A (filled squares) 23 channels in HEK293 cells. Protocols are as described in Materials and methods. Values are mean±S.E.M. (C) Time constants of inactivation were determined using Chebyshev method. A single exponential equation was sufficient to fit the current decaying phase: A $\exp[-(t-K)/\tau]+C$, where A represents current amplitude at the start of the fit, τ is the time constant of inactivation, K is the time shift, and C is a constant representing the steady state asymptote. Data represent mean±S.E.M. for n determinations as shown.

3.3. Molecular modelling

The structure of crystallized Kv1.2 provided the template for homology modelling of the domain I, II and III voltage sensors of Nav1.4 sodium channel [26]. The sequence alignment used for model generation is shown in Fig. 4A. Fig. 4B–D show the voltage sensor models. Several structural elements of the Kv1.2 voltage sensor could not be resolved in the crystal structure due to weak or absent electron density, e.g. in the S1–S2 and S3–S4 extracellular linkers [31]. While the positions of the S1 and S3 α-helices could be resolved, the resolution was not high enough in this region to determine the conformations of sidechains. Similarly, the sidechains of charged residues in S2 could not be resolved. Fortunately, the resolution of a number of S4 sidechains in the Kv1.2 structure allowed the determination of the register of this α-helix. Chains of residues in the S1, S2 and S3 helices were built into the sodium channel model with rotamers that allowed the formation of salt bridges. For example, residues D1069, E1079, R1132, R1135 and R1138 are involved in salt bridges. Residues with the corresponding charges are conserved in *Shaker* channels (Fig. 4A) and participate in electrostatic interactions *in vivo* [22–24].

In the models presented here, the sidechain of L1131 is located at the interface between the S3 and S4 helices (Fig. 4D). It is possible that mutation of L1131 to the smaller sidechain alanine could alter the packing between S3 and S4 helices. The displacement of S4 relative to S3 can potentially destabilize the conformation of the voltage sensor, particularly if electrostatic interactions between the voltage sensor helices are disrupted. In contrast, the L1137 residue is located on the opposite side of the S4 helix compared to L1131 (Fig. 4D). L1137 is not interacting with any element of the voltage sensor and its mutation would therefore not be expected to have as great an effect on the stability of this domain.

4. Discussion

The present work was focused only on S4 segments of domains I, II and III since S4 of domain IV is more involved in inactivation and its coupling to activation [34] has already been extensively studied in the past, as mentioned in Introduction. Quite recently, the role of each charged residues in DIIIS4 of skeletal muscle sodium channels has been investigated [35] and it was found that central residues (R4 and R5 in the authors' terminology) produced the greatest effects (alteration of activation parameters, depolarizing shift of the conductance *versus* voltage curve, decreased valence and slowing of kinetics). This partly justified the choice of hydrophobic residues with branched

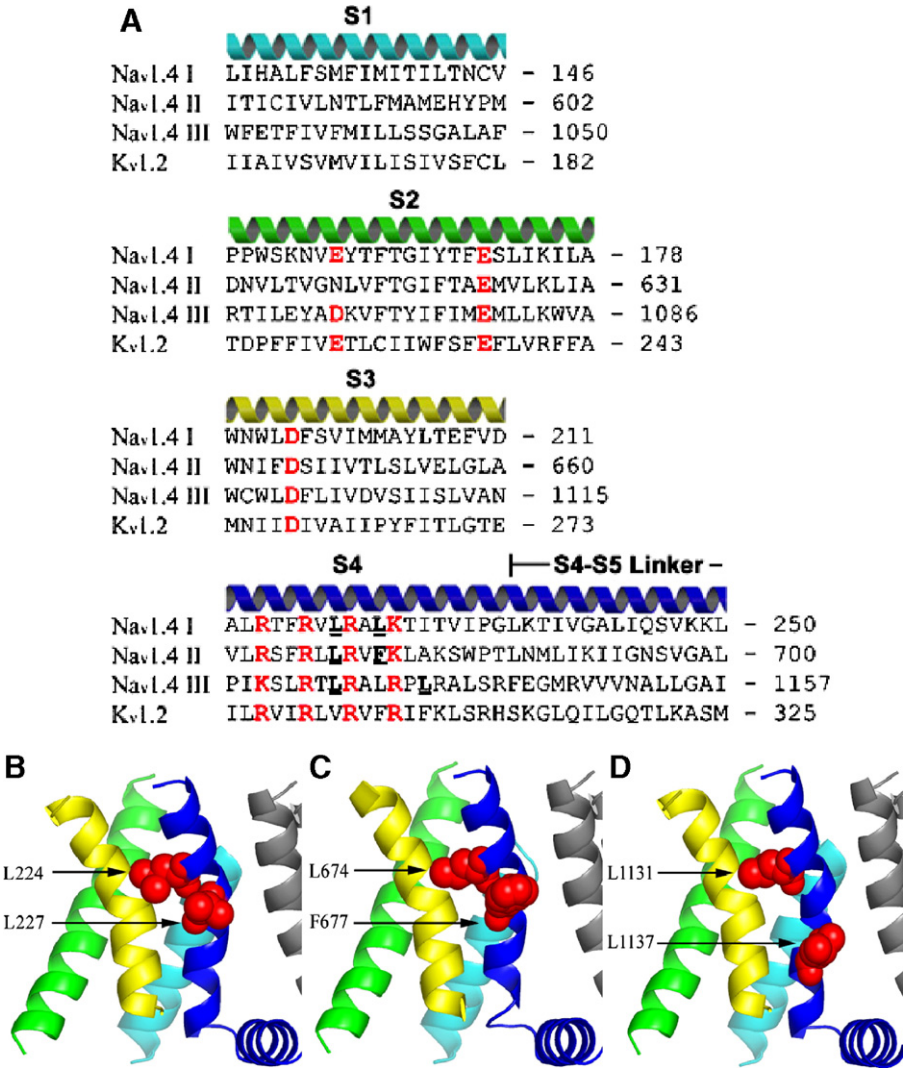

Fig. 4. Molecular modelling. (A) Sequence alignments of membrane-spanning segments S1–S4 from Kv1.2 and domains I–III of Nav1.4. The single-letter symbols for conserved charged residues are coloured red. Hydrophobic residues mutated in the course of the current study are underlined. Residue numbers are shown on the right. (B–D) are models of the Nav1.4 domain I, domain II and domain III voltage sensors, respectively. Transmembrane helices are coloured as in (A). The grey helix on the right of each model is the S5 segment from an adjacent domain. Hydrophobic residues underlined in (A) are shown in space-filling representation and coloured red.

sidechains to be substituted, next to these important charged residues. In the voltage-dependent sodium channel investigated here, DIS4, DIIS4 and DIIIS4 have four, five, and six positive charges respectively whereas DIVS4 presents 7 or 8 positively-charged residues. The lowest net charge in S4 is found in the KCNQ1, a member of a subfamily of Kv potassium channel [36]. Here we show that substitutions L224A and L227A in DIS4, as well as L674A and F677A in DIIS4 led to activation channel dysfunction, leaving inactivation parameters unaffected. The amplitude of the peak Na^+ current was not significantly changed in the mutants. However, mutation L1131A in DIIIS4 had a profound effect on channel inactivation. It should be noted that the S4 segment of domain III of the human skeletal muscle sodium channel presents 6 positive charges: K1125, R1128, R1131, R1134, R1137, and R1142, the latest being maybe 'atypical' since it does not follow the usual pattern being separated to the previous arginine by 4 residues instead of 3. Strikingly, the peptide approach with a synthetic S4 of domain III previously showed the same trend [25].

A previous work already found that comparable or even larger shifts in steady-state activation and inactivation curves are caused by substitutions of hydrophobic residues in the S4 sequence of the Shaker K^+ channel [19]. Except for the L366 mutation, midpoints of current–voltage curves as well as their slopes are differently modified depending on which hydrophobic residues are substituted. They conclude that channel activation and inactivation are coupled and suggest that the S4 structure plays a role in determining the relative stabilities of the open and closed states. In this study, six hydrophobic substitutions were tested and the effects regarding steady state activation and inactivation parameters, $V_{0.5}$ or midpoints and slopes, were significant (*e.g.* midpoints being shifted either to hyperpolarizing or depolarizing voltages depending of which residue was substituted [19]. This is in broad agreement with our findings, especially with the L1131A

mutation in domain III leading to increased inactivation time constants. In the same year (1991) as of the above mentioned study appeared another related article still on *Shaker* potassium channel. Here, the last two leucines at the C-terminal end, plus one of S4, one in the S4–S5 linker and two at the beginning of S5 were mutated to valines and also an alanine and a leucine (L3 in the authors' terminology) in the S4–S5 linker. The effects were large but again variable (either left- or right-shifts) on the activation midpoint according to the position of the mutated residues. The first phase of fast inactivation time constant was not significantly affected. It was then suggested that "leucines mediate interactions that play an important role in the transduction of charge movement into channel opening and closing" [37]. In another potassium channel (rKv1.4) and in another segment (S6), a threonine at position 529 previously shown to be a key determinant of the blocking potency of several pore blockers was mutated with Gly, Leu, Ile, Val, Ala, or Phe. Amongst the effects of these mutations, the slowing down of deactivation was largely correlated with the degree of increase in 529 sidechain hydrophobicity [38]. It was proposed that in the open state, the 529 sidechain faces a hydrophobic protein interior, as for some of the residues (like L1131) in our study which shows the largest effect in the negative shift of the fast inactivation curve as well as a significantly reduced slope (Table 2). Overall, our data further support the notion of an asymmetric sodium channel functioning, analogous to a four-stroke-four-four cylinders engine, each homologous domain underlying different aspects of channel gating. Indeed, homologous domains seem to function independently.

The Kv1.2 structure represents the first determined case of a mammalian voltage-gated channel. Kv1.2 was crystallized adopting a native conformation since the transmembrane topology corresponds with predictions made for members of the voltage-gated ion channel family. The channel structure reveals that each voltage sensor domain, formed by the S1 to S4 transmembrane helices, is packed loosely against the S5 helix of an adjacent monomer. The pore-lining S6 helices are bent and the cytoplasmic end of the pore has a diameter of ~12 Å, which suggests that the pore is in an open conformation [31]. The first four positive charges of the S4 helices, which carry most of the gating charges in *Shaker* potassium channels are located on the extracellular side of the predicted membrane region, which is consistent with the outward movement of the S4 segments during channel activation. It has been recently proposed that S4 segments move inwardly during transition to the resting closed-state conformation, applying pressure *via* the S4–S5 linkers to straighten the S6 helices with the consequent formation of a pore-blocking constriction at the pore cytoplasmic end.

Sequence alignments of the S1, S2, S3, S4 segments and the S4–S5 linker of the Kv1.2 potassium channel and the first three domains of the human skeletal sodium channel (Nav1.4) are shown in Fig. 4A. Charged residues in the S2, S3 and S4 sections that play a role in voltage sensing are conserved, which is consistent with the adoption by sodium channel voltage sensors of an equivalent activated-state conformation, as found in the Kv1.2 crystal structure. Homology models of the Nav1.4 sodium channel domain I, II and III voltage sensors (the S1–S4 helices, with the remaining segments S5, the P- loop and S5 defining the 'pore module') were generated (Fig. 4B–D, respectively) to provide visual evidence for the location of the branched hydrophobic residues (in red) which were mutated in S4s. The S3 and S4 helices are packed together in an antiparallel arrangement in Kv1.2 and in the crystal structures of the KvAP bacterial voltage-gated potassium channel and its isolated voltage sensor [39]. In the models of domains I and II Nav1.4 channels, the hydrophobic residues of interest are spatially close together and in sufficient proximity to form packing interactions with the S3 helix (Fig. 4B, C). Whereas the sidechain of L1131 is located at the interface between the S3 and S4 helices in the domain III model, the L1137 does not make contact with any other element of the channel and presumably interacts with lipid molecules in the membrane.

The model suggests that mutation of L1131 to the small side chain alanine could alter the packing between S3 and S4 helices, with a consequent disruption of interactions that stabilize conformations of the voltage sensor. In contrast, the L1137 residue is located on the S4 helix on the opposite side and is not interacting with other elements of the voltage sensor. Therefore, its mutation would not be expected to have a great effect on the stability of this domain. This modelling is consistent with the experimental results which show a greater effect of the L1131A over the L1137A on the function of Nav1.4. Greater understanding of the conformational changes the voltage sensor domain during transitions between functional states is required for more detailed studies. It would be of particular interest to determine whether the S4 helix moves together with S3 and S2, during the gating, or if they move independently. Indeed, at least one acidic residue in the latter segment of *Shaker* K^+ channels was shown to contribute significantly to the gating together with three arginines in S4 [40].

In summary, the experimental and modelling studies presented here show that a rearrangement of the voltage sensor in its activated state may play a role in the onset of channel inactivation, and mutations of the hydrophobic branched-sidechain residues on the S4 helices of domains I, II and III can hasten this conformational change.

Acknowledgements

S.B. acknowledges the support of Dr. L. Ptàcek (Department of Neurology, University of Utah, Salt Lake City) and the AFM (Association Française contre les Myopathies). A.O'R. was funded by a grant from BBSRC (UK) and thanks Pr. Wallace (Department of Crystallography, Birkbeck College, University of London, UK) for support. H.D. and S.B. are supported by the CNRS (France) and thank Dr. H. R. Leuchtag (P. O. Box 74, Bandera, Texas 78003, USA) for the initial ideas at the origin of this work.

References

[1] M. Noda, S. Shimizu, T. Tanabe, T. Takai, T. Kayano, T. Ikeda, H. Takahashi, H. Nakayama, Y. Kanaoka, N. Minamino, K. Kangawa, H. Matsuo, M.A. Raftery, T. Hirose, S. Inayama, H. Hayashida, T. Miyata, S. Numa, Primary structure of *Electrophorus electricus* sodium channel deduced from cDNA sequence, Nature 312 (1984) 121–127.

[2] D.A. Doyle, J. Morais Cabral, R.A. Pfuetzner, A. Kuo, J.M. Gulbis, S.L. Cohen, B.T. Chait, R. MacKinnon, The structure of the potassium channel: molecular basis of K+ conduction and selectivity, Science 280 (1998) 69–77.
[3] W. Stühmer, F. Conti, H. Suzuki, X.D. Wang, M. Noda, N. Yahagi, H. Kubo, S. Numa, Structural parts involved in activation and inactivation of the sodium channel, Nature 339 (1989) 597–603.
[4] K.J. Kontis, A. Rounaghi, A.L. Goldin, Sodium channel activation gating is affected by substitutions of voltage sensor positive charges in all four domains, J. Gen. Physiol. 110 (1997) 391–401.
[5] N. Yang, R. Horn, Evidence for voltage-dependent S4 movement in sodium channels, Neuron. 15 (1995) 213–218.
[6] N. Yang, A.L. George Jr., R. Horn, Molecular basis of charge movement in voltage-gated sodium channels, Neuron 16 (1996) 113–122.
[7] L.M. Mannuzzu, M. Moronne, E.Y. Isacoff, Direct physical measure of conformational rearrangement underlying potassium channel gating, Science 271 (1996) 213–216.
[8] A. Cha, G.E. Snyder, P.R. Selvin, F. Bezanilla, Atomic scale movement of the voltage-sensing region in a potassium channel measured via spectroscopy, Nature 402 (1999) 809–813.
[9] K.S. Glauner, L.M. Mannuzzu, C.S. Gandhi, E.Y. Isacoff, Spectroscopic mapping of voltage sensor movement in the Shaker potassium channel, Nature 402 (1999) 813–817.
[10] F.H. Yu, W.A. Catterall, Overview of the voltage-gated sodium channel family, Genome Biol. 4 (2003) 200–207.
[11] L. Ptácek, A.L. George Jr., R.L. Barchi, R.C. Griggs, J.E. Riggs, M. Robertson, M.F. Leppert, Mutations in an S4 segment of the adult skeletal muscle sodium channel cause paramyotonia congenita, Neuron 8 (1992) 891–897.
[12] J. Wang, V. Dubowitz, F. Lehmann-Horn, K.L. Ricker, E.P. Hoffman, In vivo sodium channel structure/function studies: consecutive Arg 1448 changes to Cys, His, and Pro at the extracellular surface of IVS4, Soc. Gen. Physiol. Ser. 50 (1995) 77–88.
[13] K. Jurkat-Rott, N. Mitrovic, C. Hang, A. Kouzmekine, P. Iaizzo, J. Herzog, H. Lerche, S. Nicole, J. Vale-Santos, D. Chauveau, et al., Voltage-sensor sodium channel mutations cause hypokalemic periodic paralysis type 2 by enhanced inactivation and reduced current, Proc. Natl. Acad. Sci. U. S. A. 97 (2000) 9549–9554.
[14] S. Bendahhou, T.R. Cummins, R.C. Griggs, Y.H. Fu, L.J. Ptácek, Sodium channel inactivation defects are associated with acetazolamide-exacerbated hypokalemic periodic paralysis, Ann. Neurol. 50 (2001) 417–420.
[15] M. Chahine, A.L. George, M. Zhou, S. Ji, W. Sun, R.L. Barchi, R. Horn, Sodium channel mutations in paramyotonia congenita uncouple inactivation from activation, Neuron 12 (1994) 281–294.
[16] J.A. Morrill, R.H. Brown Jr., S.C. Cannon, Gating of the L-type Ca channel in human skeletal myotubes: an activation defect caused by the hypokalemic periodic paralysis mutation R528H, J. Neurosci. 18 (1998) 10320–10334.
[17] N. Mitrovic, A.L. George Jr., R. Horn, Role of domain 4 in sodium channel slow inactivation, J. Gen. Physiol. 115 (2000) 707–718.
[18] V.J. Auld, A.L. Goldin, D.S. Krafte, W.A. Catterall, H.A. Lester, N. Davidson, R.J. Dunn, A neutral amino acid change in segment IIS4 dramatically alters the gating properties of the voltage-dependent sodium channel, Proc. Natl. Acad. Sci. U. S. A. 87 (1990) 323–327.
[19] G.A. Lopez, Y.N. Jan, L.Y. Jan, Hydrophobic substitution mutations in the S4 sequence alter voltage-dependent gating in Shaker K+ channels, Neuron 7 (1991) 327–336.
[20] K. Yoshino, T. Sakurai, IV Ferroelectric liquid crystals and their chemical and electrical properties, in: J.W. Goodby, et al., (Eds.), Ferroelectric Liquid Crystals: Principles, Properties and Applications, Gordon and Breach, 1991, pp. 317–363.
[21] H.R. Leuchtag, Indications of the existence of ferroelectric units in excitable membrane channels, J. Theor. Biol. 127 (1987) 321–340.
[22] D. Papazian, Atomic proximity between S4 segment and pore domain in Shaker potassium channels, Neuron 39 (2003) 467–481.
[23] S.H. Tiwari-Woodruff, M.A. Lin, C.T. Schulteis CT, D.M. Papazian, Voltage-dependent structural interactions in the Shaker K+ channel, J. Gen. Physiol. 115 (2000) 123–138.
[24] T. Hessa, S.H. White, G. von Heijne, Membrane insertion of a potassium-channel voltage sensor, Science 307 (2005) 1427.
[25] O. Helluin, M. Beyermann, H.R. Leuchtag, H. Duclohier, A critical role for the branched sidechain adjacent to the third arginine of the sodium channel voltage sensor. A peptide approach, IEEE Trans. Dielectr. Electr. Insul. 8 (2001) 637–648.
[26] S.B. Long, E.B. Campbell, R. MacKinnon, Crystal structure of a mammalian voltage-dependent Shaker family K+ channel, Science 309 (2005) 897–903.
[27] S. Bendahhou, T.R. Cummins, R. Tawil, S.G. Waxman, L.J. Ptácek, Activation and inactivation of the voltage-gated sodium channel: role of segment S5 revealed by a novel hyperkalaemic periodic paralysis mutation, J. Neurosci. 19 (1999) 4762–4771.
[28] F.L. Graham, A.J. Van Der Eb, A new technique for assay for infectivity of human adenovirus 5 DNA, Virology 52 (1973) 456–467.
[29] G. Sarkar, G.S.S. Sommer, The "megaprimer" method of site-directed mutagenesis, BioTechniques 8 (1990) 404–407.
[30] O.P. Hamill, A. Marty, E. Neher, B. Sakmann, F.J. Sigworth, Improved patch-clamp techniques for high-resolution current recording from cells and cell-free membrane patches, Pflügers Arch. 391 (1981) 85–100.
[31] S.B. Long, E.B. Campbell, R. MacKinnon, Voltage sensor of Kv1.2: structural basis of electromechanical coupling, Science 309 (2005) 903–908.
[32] J.D. Thompson, D.G. Higgins, T.J. Gibson, CLUSTAL W: improving the sensitivity of progressive multiple sequence alignment through sequence weighting, position-specific gap penalties and weight matrix choice, Nucleic Acids Res. 22 (1994) 4673–4680.
[33] M. Clark, R.D. Cramer, N. van Opdenbosch, Validation of the general purpose Tripos 5.2 force field, J. Comput. Chem. 10 (1989) 982–1012.
[34] F.J. Kuhn, N.G. Greeff, Movement of voltage sensor S4 in domain 4 is tightly coupled to sodium channel fast inactivation and gating charge immobilization, J. Gen. Physiol. 114 (1999) 167–183.
[35] J.R. Groome, H.A. Alexander, E. Fujimoto, M. Sherry, D. Petty, Central charged residues in DIIIS4 regulate deactivation gating in skeletal muscle sodium channels, Cell. Mol. Neurobiol. 27 (2007) 87–106.
[36] G. Panaghie, G.W. Abbott, The role of S4 charges in voltage-dependent and voltage-independent KCNQ1 potassium channel complexes, J. Gen. Physiol. 129 (2007) 121–133.
[37] K. McCormack, M.A. Tanouye, L.E. Iverson, J-Y. Lin, M. Ramaswami, T. McCormack, J. Campanelli, M.K. Mathew, B. Rudy, A role for hydrophobic residues in the voltage-dependent gating of Shaker K^+ channels, Proc. Natl. Acad. Sci. U. S. A. 88 (1991) 2931–2935.
[38] Y.-Y. Zhou, M. Jiang, S. Ling, G.-N. Tseng, Stabilization of a channel's open state by a hydrophobic residue in the sixth membrane-spanning segment (S6) of rKv .4, Pflügers Arch.-Eur. J. Physiol. 437 (1998) 114–122.
[39] Y. Jiang, A. Lee, V. Ruta, M. Cadene, B.T. Chait, X-ray structure of a voltage-dependent K+ channel, Nature 423 (2003) 33–41.
[40] S.A. Seoh, D. Sigg, D.M. Papazian, F. Bezanilla, Voltage-sensing residues in the S2 and S4 segments of the Shaker K^+ channels, Neuron 16 (1996) 1159–1167.